Thermal Decomposition Mechanism of Metal Xanthate to Metal Sulfide Nanoparticles in Ammonia Solution

H L Lian, Q Shen, Y J Fan, L M Wu and Z X Sun*

School of Chemistry and Chemical Engineering, University of Jinan, 250022 Jinan, China

Corresponding author and e-mail: Z X Sun, sunzx@ujn.edu.cn

Abstract. Synthesizing metal sulfide nanoparticle by thermally decomposing metal xanthate is a facile method; however, the proposed mechanism rationalized by Chugaev reaction has not been experimentally proved. Herein we report our experimental evidence to elucidate the reaction mechanism. In this study, ZnS and CdS nanoparticles of a few nanometers in size were prepared by thermal decomposition of a single source precursor of metal xanthates in ammonia solution at temperature as low as 90°C. The particle size and crystallinity were characterized using XRD techniques. The decomposition mechanism studied by UV spectra in combination with GC-MS and FTIR is fund to be a nucleophilic elimination reaction with main products of MS nanoparticles, alkanols, manothiocarbonate, carbonyl sulfide and dixanthogen. Olefin, a main product of Chugaev reaction, is not detected in this process, which suggests that the thermal decomposition mechanism of MX_2 to MS is not that of Chugaev reaction.

1. Introduction

Metal sulfide such as ZnS and CdS semiconductor nanoparticles (NP) as advanced materials has attracted much research attention due to their wonderful size-dependent tunable optical properties [1]. As a semiconductor compound, ZnS or CdS and their mutual core shell structure possesses photoluminescence (PL) and electroluminescence (EL) and have applied as sensors and lasers [2], light-emitting diodes when doped [3, 4], solar cells [5], catalysts [6]. In past years, synthesizing ZnS or CdS using single source precursor of metal chalcogenide compound has been explored, the results is encouraging. O'Brien's group reported their results for the synthesis of CdS nanoparticles [7]. Efrima's group synthesized a series of metal sulfide NP, the thermal decomposition mechanism of the chalcogenide precursor was theoretically rationalized using the Chugaev reaction [1,8]. This mechanism is accepted by some researchers when they prepare NiS NP [9]. However no experimental evidence of the formation of olefin was provided in all these studies. On the other hand different mechanism for thermal decomposition of single precursor of metal chalcogenide was also proposed [10], in which the decomposition products were thiourea, hydrogen sulfide and solid metal sulfide nanoparticles. Apparently people's concerns over the thermal decomposition of single precursor of metal chalcogenide are inconsistent and a generalized mechanism has not yet been commonly accepted. We used a single source precursor of cadmium xanthates with variable carbon chain length in an ammonia solution to synthesis size tunable CdS nanoparticles, and the

Lian, H., Shen, Q., Fan, Y., Wu, L. and Sun, Z.
Thermal Decomposition Mechanism of Metal Xanthate to Metal Sulfide Nanoparticles in Ammonia Solution.
In *Proceedings of the International Workshop on Materials, Chemistry and Engineering (IWMCE 2018)*, pages 268-275
ISBN: 978-989-758-346-9

experimental results didn't support the hypothesis based on Chugaev reaction [11]. Neither did a published paper using metal xanthate as a precursor to prepare highly luminescent quantum dot of metal sulfide [12].

In order to understand the thermal decomposition mechanism of the metal xanthate in ammonia solution further, we used zinc or cadmium xanthate as a single source precursor to prepare ZnS or CdS NP and the process is inspected respectively by UV, FTIR and GC –MS spectroscopic techniques.

2. Experimental

2.1. Material and methods

Zinc acetate, potassium hydroxide, potassium n-heptylxanthate, ethanol, acetone, petroleum, aqueous ammonia, ether and other chemicals used in the present study were all reagent grade and all water used in the experiments was deionized distilled water.

The ZnS and CdS powders produced were characterized by X-ray diffraction (XRD) using a Bruker D8-Advance X-ray diffractometer employing Cu Kα radiation (wavelength 1. 54 Å). A continuous mode was used for collecting data from 10° to 80° of 2θ at a scanning rate $0.1°•S^{-1}$.

A Shimadzu UV-2450 UV-visible (UV-vis) spectrophotometer and a Bruker VERTEX-70 FTIR was used to carry out optical measurements and to follow the thermolysis of the samples. Samples were placed in quartz cuvettes (1 cm path length).

GC-MS analyses were performed on a Thermo Electron DSQ quadrupole mass spectrometer connected directly to a Thermo Electron Focus gas chromatograph and to an autosampler AS 3000 (Thermo Electron, Dreieich, Germany). A fused-silica capillary column Optima-17 (15 m × 0.25 mm i.d., 0.25 μm film thickness) from Macherey-Nagel (Düren, Germany) was used. The gas over reaction liquid was collected using a 1 mL injecting syringe and measurements were performed by selected-ion monitoring (SIM) of m/z 240 for d0-ethanol and m/z 245 for d6-ethanol with a dwell time of 50 ms for each ion. The following oven temperature program was used with helium as the carrier gas at a constant flow rate of 1 mL min^{-1}: 1 min at 70 °C, then increased to 180 °C at a rate of 30 °C min^{-1}, and to 280 °C at a rate of 70 °C min^{-1}; the oven temperature of 280 °C was held for 1 min. Interface, injector and ion source were kept at 280 °C, 200 °C and 250 °C, respectively. Electron energy and electron current were set to 70 eV and 100 μA, respectively, for electron-capture negative-ion chemical ionization (ECNICI) with methane as the reagent gas at a flow rate of 2.4 mL min^{-1}.

2.2. Synthesis of ZnX_2 and CdX_2

After dissolving 0.02 mol K ($CH_3(CH_2)_6OCS_2$) in distilled water, 100 mL solution (containing 0.013 mol zinc acetate) was drop wise added. Then a white precipitate appeared. After the reaction completed, the product was centrifuged at 7000 rpm for 10 min, rinsed three times with a ethanol solution (the volume ratio of water and ethanol was 3:1) to yield purified $Zn(CH_3(CH_2)_6OCS_2)_2$.

2.3. Synthesis of ZnS or CdS by the thermal decomposition of ZnX_2 or CdX_2.

In a flask containing 60 mL ammonia solution and placed in an oil bath heated up to 90℃, 300mg $Zn(CH_3(CH_2)_6OCS_2)_2$ was added to the flask with stirring, after refluxing for 8 hours to decompose the ZnX_2 completely. The solution was cooled gradually at room temperature and then the supernatant separated from the solid particles. The deposits was collected by centrifugation at 7000 rpm for 10 min and washed three times with ethanol and water.

3. Results and discussions

The X-ray diffraction results are shown in Figure 1.

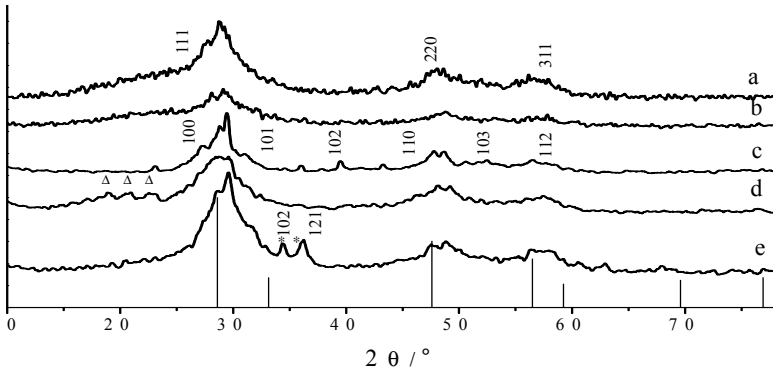

Figure 1. XRD data for zinc sulfide prepared by decomposing zinc n- heptylxanthate in alkaline. Solution of ammonia or sodium hydroxide at different reaction time at 90°C.(a: 5 h; b: 9 h; c: 15 h; in ammonia solution at pH about 13.4). (d: yellowish solid; e: 9 h; in sodium hydroxide solution at pH about 12.2). (* is $NaZnO_2$; Δ may be from heptyldixanthogen)

Diffraction peaks at 2 θ values between 25.0~35.0°, 45.0~50.0°, and 55.5~60.5° can be clearly seen in Figure 1 curve a, which is indexed as the (111), (220), and (311) plane of zinc sulfide respectively. However, the (100), (101), (102), (103) plane of wurtzite ZnS appears in the curve c after reacting for 15 hours, indicating the presence of hexagonal wurtzite ZnS as well. When solution pH increases less than 13, a yellowish solid can be yield. In order to explore the mechanism, we did another parallel experiment, in which we use sodium hydroxide as the nucleophilic agent to attack the most electrons deficient C-S bonds in ZnX_2 to yield zinc sulfide. The XRD results are shown in Figure 1. curve e. The curve d is yellowish solid produced in ammonia and zinc sulfide in sodium hydroxide solution, respectively. Diffraction peaks at 2 θ values between 25.0~35.0°, 45.0~50.0°, and 55.5~60.5°, identified as the (111), (220), and (311) peaks of zinc sulfide can be clearly seen. However, some weak peaks at 2 θ values between 15.0~25.0°, 33.2~35.5°, 36.0~38.0° can also be seen. The peaks at 15.0~25.0° may be identified as the dixanthogen's diffraction peaks. And the others can be identified as the (102), (121) peaks of $NaZnO_2$ which could be produced by the side reaction during the thermal decomposition process of ZnX_2 in sodium hydroxide solution. The crystallite size was calculated here using Scherrer's equation:

$$d = K\lambda/(\beta\cos\theta) \quad (1)$$

where d is the crystal size, the X-ray wavelength, the broadening of the diffraction peak and θ the diffraction angle. The sizes of the crystallites determined according to the broadening of (111) diffraction plane of the ZnS crystal are 3.2, 3.8, 4.3 nm for a, b, c and 3.1 nm, 3.9 nm for d, e respectively. Obviously, the particle size of formed ZnS increases progressively with increasing reaction time. XRD data for cadmium sulfide prepared by decomposing variable cadmium xanthates in ammonia solution has been reported in a previews paper of ours [11], which proved the thermal decomposition products were size variable CdS NPs, therefore not repeat here.

In order to find out the thermal decomposition mechanism of zinc and cadmium xanthates in alkaline solution, the solution samples at different reaction time were carefully analyzed using UV technique, the measurement results of UV spectra are shown in Figure 2, in which the UV absorption spectra of ZnX_2 and CdX_2 in ammonia solution at 90°C are measured with varying time.

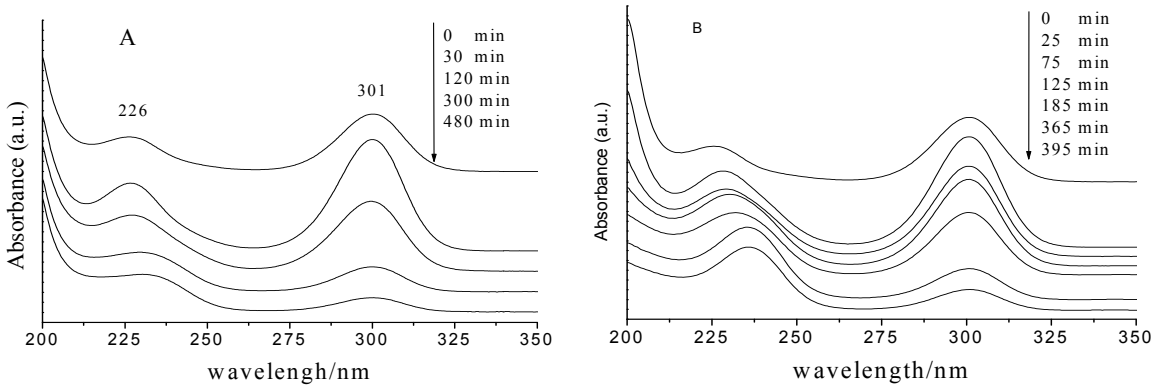

Figure 2. UV absorption spectra for zinc sulfide and cadmium sulfide prepared by decomposing ZnX_2 or CdX_2 with different reaction time at 90°C (where from top to bottom denote 0 min, 30 min, 120 min, 300 min and 480 min in Figure 2A for ZnX_2, and 0 min, 25 min, 75 min, 125 min, 195 min, 365 min and 395 min in Figure 2B for CdX_2 respectively).

From Figure 2 we can see the absorbance peak at 301 nm is increasing in the first 30 min for both ZnX_2 and CdX_2 suspension, indicating the concentration of xanthate is increasing i.e. xanthate is releasing from the metal xanthate to solution. With increasing reaction time, the peak at 301 nm decreased progressively in both ZnX_2 and CdX_2 suspensions, suggested the xanthates released from metal xanthate were consuming gradually together with the formation of the metal sulfide nanoparticles, meanwhile the absorbance peak at 226 nm shows a few wavelengths red shift. After closely evaluating the red shift we found out that the final peak actually comes from the combination of three peaks i.e. a peak at 222 nm, a peak at 226 nm and a peak at 238 nm after simulating. As a typical example, Figure 3 shows the simulated peaks for UV spectra for CdX_2 after reacting for 365 min at 90°C in ammonia solution.

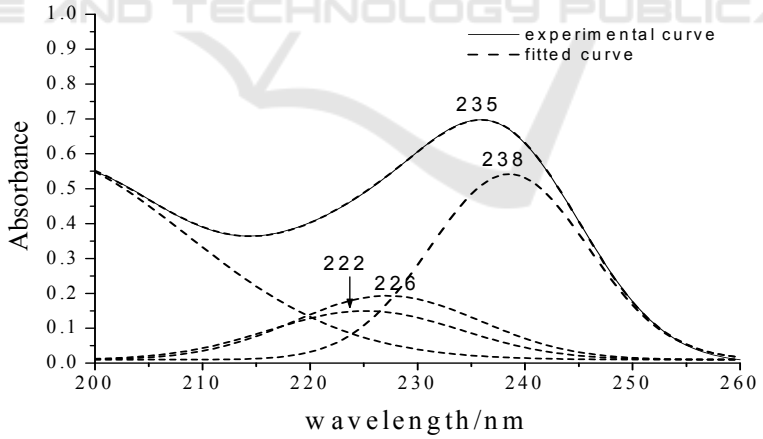

Figure 3. Simulated peaks for UV spectrum for CdX2 after reacting for 365 min at 90°C in ammonia solution (the solid line denotes the recorded UV spectrum; dashed lines denote simulated peaks). The four curve fitted sub-peaks (dashed lines) shown resulted in the sum of squares (SS) of 0.00051.

The curve fitted sub-peak was located at 222 nm, 226 nm and 238 nm respectively. The peak at 222 nm and the peak at 238 nm belong to the absorbance from monothiocarbonate and dixanthogen respectively [13]. In the same way, we simulated the UV spectra for ZnX_2 after reacting 30, 120, 300 and 480 min and for CdX_2 after reacting for 25, 75, 125, 185 and 395 min respectively at 90°C in ammonia solution, the results are presented in Table 1. From Table 1 we can see that with increasing

reaction time, the peak intensity at 226 nm attributed to xanthate increased in the first 30 min and then decreased continuously in line with that at 301 nm shown in Figure 2. Apparently the variations of the peak at 301 nm and simulated peak at 226 nm show the same trend, implying xanthate is one of the thermal decomposition products of metal xanthate. At the same time, the simulated peak at 238 nm attributed to dixanthogen increased at the first 300 min and then shown somewhat decreasing, indicating dixanthogen is one of the thermal decomposition products. However, the simulated peak at 222 attributed to monothiocarbonate shown some different phenomena for ZnX_2 and CdX_2 system. In ZnX_2 suspension, it increased at the first 5h and then stabilized. In CdX_2 system, however, it increased at the first 2h and then decreased irregularly, which may indicate to some extent different intermediate thermal decomposition process for ZnX_2 and CdX_2 system. These phenomena may reveal that the monothiocarbonate may be an intermediate thermolysis product, which then goes through further decomposition.

Table 1. Variations of UV absorbance in ZnX_2 or CdX_2 suspension during the thermal decomposition process.

precursor	Time/min	Wavelength/nm			Sum of squares
		222	226	238	
ZnX_2	0	---	0.35	---	
	30	0.08	0.45	0.10	0.043
	120	0.15	0.37	0.17	4.33E-4
	300	0.32	0.04	0.19	1.03E-5
	480	0.31	0	0.17	5.57E-5
CdX_2	0	--	0.36	--	
	25	0.10	0.57	0.15	0.00862
	75	0.15	0.53	0.27	0.0472
	125	0.26	0.25	0.38	5.83E-4
	185	0.13	0.22	0.47	0.010033
	365	0.14	0.19	0.54	5.1E-4
	395	0.06	0.12	0.53	0.00132

Whenever dealing with the thermolysis of xanthate, people naturally tend to consider it as a well known Chugaev reaction. Efrima's group has rationalized the thermal decomposition mechanism of various metal xanthates in alkylamine solution using Chugaev reaction.[1] In order to test the applicability of Chugaev reaction in explaining the reaction mechanism in our system, we made great effort to find out the evidence of olefin, as the main thermal decomposition product of Chugaev reaction is olefin and if it is there, it should be easily identified by gas chromatography in combination with mass spectroscopy (GC-MS) and FTIR measurements. However, the measurements results didn't show any evidence of olefin, but different degradation products of xanthate (supporting information, Figure S1-S2), which is consistent with the results of our UV spectroscopic measurements. From the results of FTIR measurements, we can find a peak at wave number of 2053 cm^{-1}, due to the asymmetric stretching vibration from the carbonyl sulfide. From the results of GC-MS measurements, the peak at retention time of 1.428 min is assigned as that from CS_2, in which 76, 44, 32 corresponds respectively to the mass spectrum of CS_2, CS and S. From the mass spectra at retention time of 1.428 min, we can also see the mixed mass spectra of air and carbonyl sulfide with m/z=60, 44, 32, 28, 16, 12, m/z=60 is COS and m/z=44, 32, 28 can be attributed to the degradation products of COS and their mixture with CO_2, O_2 and N_2. The experimental results of this GC-MS measurement can evidence the existence of COS, which is in consistence with the results of FTIR measurements.

In order to confirm what else the yellowish solid shown in Figure 1 contains, we measured its FTIR and UV spectra, the results are shown in Figure 4.

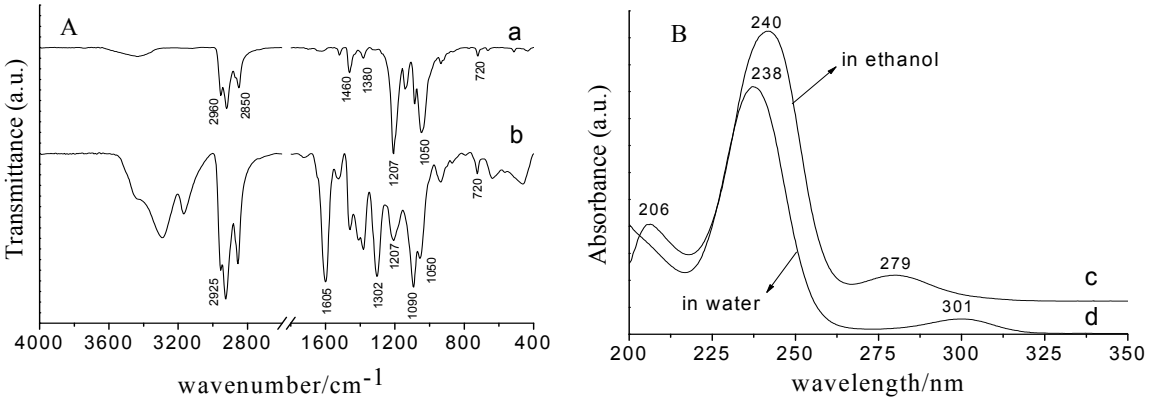

Figure 4. IR and UV absorption spectra for zinc sulfide prepared by decomposing ZnX_2 at 90°C (where (a) ZnX_2; (b) the yellowish solid on the **surface** of ZnS; (c) yellowish solid in ethanol solution; (d) yellowish solid in water solution).

In Figure 4A, the curve 'a' is ZnX_2 and the curve 'b' is the yellowish solid sample. In the range from 3000 to 2800 cm^{-1}, characteristic bands for carbon-hydrogen vibrations are seen. The peaks around 2960 and 2925 cm^{-1} are the asymmetric methyl (CH_3) and methylene (CH_2) vibration bands, respectively; and the bands around 2870 and 2850 cm-1 are the corresponding symmetric vibrations. The two sets of absorption bands between 1360 and 1390 cm^{-1} as well as between 1420 cm^{-1} and 1480 cm^{-1} are due to C-H bending modes and appear in a similar position, to a greater or lesser extent, in all of the FTIR spectra shown in Figure 4A. The band at 1200 cm^{-1} is mainly due to the asymmetric stretching vibration of C-O-C, and the band between 1064 and 1021 cm^{-1} has a strong involvement of the asymmetric S-C-S stretch [14, 15]. According to the curve 'b', the peaks at 1605 and 1090 cm^{-1} are the characteristic bands for O-heptyl monothiocarbonate group (R-O-C(O)-S-). The set of absorption band at 1605 cm^{-1} is due to the stretch vibration of carbonyl group (C=O) and the peaks around 1190 cm-1 is the asymmetric stretch vibration of -C-O-C- group. The peaks at 1302, 1207 and 1050 cm^{-1} are the characteristic bands for n-heptyldixanthate.

Figure 4B is UV absorbance spectra for the solution of the yellowish solid sample in water and in ethanol solution, respectively. As we know that n-heptyldixanthogen is hydrophobic and can easily dissolve in ethanol and hardly in water. Clearly the peaks at 240 nm and 279 nm in ethanol solution and 238 nm in water of n-heptyldixanthogen can be seen [12]. The peak at 206 nm attributes to CS_2 produced by the decomposition of the remained n-heptylxanthate.

According to the Chugaev reaction, Pradhan and Efrima proposed a mechanism including decomposition products of metal sulfide, carbonyl sulfide, olefins and xanthic acid.1 However, the decomposition products in our system are xanthate, monothiocarbonate, carbonyl sulfide and dixanthogen, which suggested that Chugaev reaction cannot account for the decomposition mechanism of metal xanthate in this system.

According to the decomposition products observed we suggest that the decomposition of MX_2 via three steps, which is schematically illustrated in Figure 5. Our proposed mechanism was partly supported by some evidences proposed by Jones and Woodcock in 1982 [16], when they tried to understand the reaction mechanism of xanthate in mineral flotation.

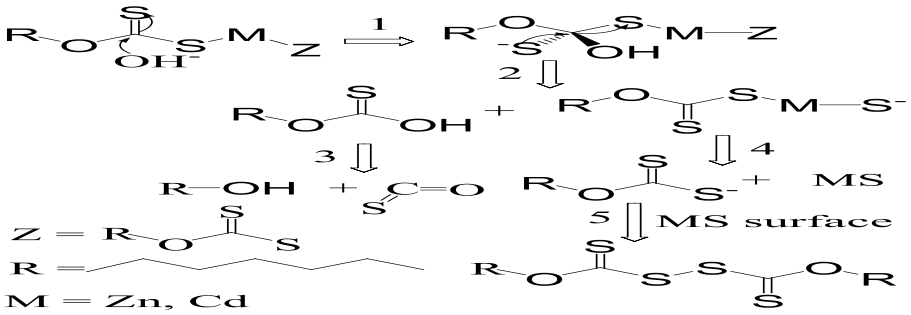

Figure 5. The thermal decomposition mechanism of ZnX_2 and CdX_2 in ammonia solution.

Firstly, the NH_3, OH^- might attack the O-C-S_2Zn group, moving negative charge from OH^- toward the C=S bond. Then the S-M-Z group estranged from MX_2 and formed Z-M-S^-, and the remaining was R-O-C(S)-OH. Secondly, the groups can decompose sequentially. As the group R-O-C(S)-OH breaks down; O-C-S and n-hepthanol emerged. The Z-M-S^- group further decomposes into metal sulfide and n-heptylxanthate anion. However, the reaction will continue if solution pH is lower than 13. At last the dixanthogen will be formed by the reaction shown in Figure 5. Double groups of $ROC(S)S^-$ can be oxidized into n-heptyl dixanthogen on the surface of the zinc sulfide.

4. Conclusions

Following conclusions can be drawn from this investigation.

1. The size of cubic MS particles is between 3 nm and 4.1 nm by a thermolysis method of a single source precursor of MX_2.
2. The decomposition process of MX_2 is a nucleophilic reaction and NH_3 and OH^- act as powerful nucleophilic agents in the reaction.
3. The decomposition products contain zinc sulfide, xanthate, O-heptyl monothiocarbonate, carbonyl sulfide, heptanol and dixanthogen.

Acknowledgments

Financial support from Chinese Natural Science Foundation (No. 51274104; No. 50874052), National Basic Research Program of China (No. 2011CB933700) is gratefully acknowledged.

References

[1] Pradhan N, Katz B and Efrima S 2003 *J. Phys. Chem. B* **107** 13843
[2] Tanne J, Schäfer D, Khalid W, Parak W J and Lisdat F 2011 *Anal. Chem*. **83** 7778
[3] Fang X M, Roushan M, Zhang R B, Peng J, Zeng H P and Li J 2012 *J. Chem. Mater*. **24** 1710
[4] Yin X J, Xie G H, Peng Y H, Wang B W, Chen H, Li S Q, Zhang W H, Wang L and Yang C L 2017 *Adv. Funct. Mater.* **27** 1700695
[5] Yu X Y, Liao J Y, Qiu K Q, Kuang D B and Su C Y 2011 *ACS NANO*. **5** 9494
[6] Zong X, Han J F, Ma G J, Yan H J, Wu G P and Li C 2011 *J. Phys. Chem. C.* **115** 12202
[7] Nair P S, Radhakrishnan T, Revaprasadu N, Kolawole G and O'Brien P 2002 *J. Mater. Chem.* **12** 2722
[8] O'Connor G L and Nace H R 1953 *J. Am. Chem. Soc.* **75** 2118
[9] Alam N, Hill M S, Kociok G, Zeller M, Mazhar M and Molloy K C 2008 *Chem. Mat.* **20** 6157
[10] Jung Y K, Kim J I and Lee J K 2009 *J. Am. Chem. Soc.* **132** 178
[11] Zhang W M, Sun Z X, Hao W, Su D W and Vaughan D 2011 *Mater. Res. Bull.* **46** 2266
[12] Todescato F, Chesman A, Martucci A, Signorini R and Jasieniak J J 2012 *Chem. Mater.* **24** 2117
[13] Shankaranarayana M L and Patel C C 1961 *Can. J. Chem.* **39** 2590

[14] Ihs A, Uvdal K and Liedberg B 1993 *Langmuir* **9** 733
[15] Fredriksson A and Holmgren A 2007 *Colloids Surf. A.* **302** 96
[16] Jones M H and Woodcock J T 1983 *Int. J. Miner. Process.* **10** 1